

Balancing Safety and Optimality in Robot Path Planning: Algorithm and Metric

Jatin Kumar Arora^a, Soutrik Bandyopadhyay^a, Sunil Sulania^b, Shubhendu Bhasin^a

^a*Department of Electrical Engineering, Indian Institute of Technology-Delhi, Delhi, India*

^b*Samsung R&D Institute, Delhi, India*

Abstract

Path planning for autonomous robots faces a fundamental trade-off between path length and obstacle clearance. While existing algorithms typically prioritize a single objective, we introduce the Unified Path Planner (UPP), a graph-search algorithm that dynamically balances safety and optimality via adaptive heuristic weighting. UPP employs a local inverse-distance safety field and auto-tunes its parameters based on real-time search progress, achieving provable suboptimality bounds while maintaining superior clearance. To enable rigorous evaluation, we introduce the OptiSafe index, a normalized metric that quantifies the trade-off between safety and optimality. Extensive evaluation across 10 environments shows that UPP achieves a 0.94 OptiSafe score in cluttered environments, compared with 0.22-0.85 for existing methods, with only 0.5-1% path-length overhead in simulation and a 100% success rate. Hardware validation on TurtleBot confirms practical advantages despite sim-to-real gaps.

Keywords: Path planning, safety, autonomous robots

1. Introduction

The increasing integration of robots into complex human environments has made robust and efficient path planning a cornerstone of modern robotics. To ensure smooth, safe, and productive operation from autonomous vehicles Paden et al. (2016); Li et al. (2015); Lee et al. (2014) and UAVs Bortoff (2000) to robotic arms Dai et al. (2022); Korayem et al. (2011); Kim and Shin (1985); Klanke et al. (2006) and warehouse automation systems Hvezda et al. (2018); Vivaldini et al. (2010), robots must navigate dynamic and cluttered spaces effectively. To navigate effectively in the real world, planners should find safe paths without compromising optimality. However, current planners focus either on optimality or safety, prioritizing one at the expense of the other. Finding a path that is both safe and near optimal remains an unresolved challenge in cluttered environments.

Path planning algorithms span multiple families, each with distinct trade-offs. Grid-based search algorithms, such as A* Hart et al. (1968), form a foundational category. Innovations in this area include modifications to accelerate search time at the cost of optimality Warren (1993) and techniques for planning over continuous grid edges to produce shorter paths Nash and Koenig (2013). For dynamic environments, replanning algorithms like D* Stentz (1994) have been developed to efficiently update paths without recalculating from scratch. Sampling-based algorithms like the Rapidly Exploring Random Tree (RRT) Noreen et al.

(2016) have revolutionized planning in high-dimensional configuration spaces. Subsequent variants, such as RRTSmart Nasir et al. (2013), introduced intelligent sampling and path optimization to improve convergence and cost, while FASTRRT Wu et al. (2021) significantly reduced execution time through advanced sampling and steering strategies. Combinatorial methods LaValle (2006); Jafarzadeh and Fleming (2018); Ayawli et al. (2019), such as those based on Voronoi diagrams Ayawli et al. (2019), focus on maximizing path safety by maintaining the largest possible distance from obstacles. Furthermore, potential field-based methods Hwang and Ahuja (1992); Rostami et al. (2019); Azzabi and Nouri (2019) draw inspiration from physics, using attractive and repulsive forces to guide the robot. Modified versions of these algorithms have successfully addressed classic problems, such as avoiding local minima.

These algorithms excel at single objectives, A* variants optimize path length, while Voronoi-based methods maximize clearance; but lack adaptive mechanisms to jointly balance them. Existing hybrid approaches suffer from (1) hand-tuned parameters requiring manual adjustment per environment, (2) excessive conservatism in cluttered spaces, or (3) no theoretical guarantees on path cost. Recent research has made significant strides toward bridging this gap. Chu et al. (2024) proposed Optimized A*, an improved A* with turning and obstacle penalty terms, but its handcrafted cost may sacrifice path optimality for small safety gains or still cut too close to obstacles in cluttered, narrow regions. Control Barrier Functions (CBFs) have been integrated into planners like CBF-RRT Manjunath and Nguyen (2021) to enforce safety-critical constraints, demonstrating superior performance over other RRT-based methods in generating safe paths. It ensures safety but struggles with exploration under CBF constraints. SDF A* Wang et al. (2023) leverages a Signed Distance Function (SDF) to embed safety information directly into the planning process, showing significant improvements in both safety and exploration compared to traditional algorithms, but it becomes overly conservative. FS Planner Cobano et al. (2025) uses an integrated inverse distance between nodes on lazy theta A* and also gives a limit on the maximum neighbors explored in the goal and safe direction. However, this bias can miss good paths in tight passages and offers little guarantee of near-optimal path cost. Despite these advancements, existing solutions that address both objectives often come with significant drawbacks. They can incur a large trade-off that excessively penalizes path cost for minor gains in safety, or rely on fixed, non-tunable safety margins that cannot adapt to changing operational needs.

Another limitation in existing research is the evaluation methodology used by path planners. Most studies report performance using isolated metrics, such as path length or minimum clearance. While individually informative, these metrics do not capture the underlying trade-off between safety and optimality, allowing planners to appear effective by excelling in one dimension while performing poorly in the other. This fragmentation makes it challenging to compare safety-aware planners fairly or understand how algorithmic choices influence real-world safety.

To address the fundamental challenge of balancing safety and optimality in robotic path planning, we present an integrated framework that spans planning and evaluation. At its core, we introduce the Unified Path Planner (UPP), a safety-aware graph search algorithm that embeds obstacle proximity directly into the heuristic via a locally computed inverse-distance safety field, enabling simultaneous optimization of safety and path length. Crucially, unlike existing safety-aware planners that rely on fixed, hand-tuned parameters or conser-

vative inflation schemes, to the best of our knowledge, UPP is the first to combine online auto-tuning of the safety–optimality trade-off with a formally derived sub-optimality bound, ensuring theoretical bounds with adaptivity. As balancing optimality and safety is essential in robotics, we propose the OptiSafe Index. This unified and normalized metric jointly measures the balance and strength of safety and optimality in a single score. Extensive simulation studies and real-world TurtleBot experiments demonstrate that this combined approach reveals safety-optimality trade-offs that conventional planners typically do not consider.

2. Preliminaries

For the planning problem, let us consider G to be an undirected graph with the set of nodes

$$N \triangleq \{n_i \mid i = 1, 2, \dots, K\}, \quad K \in \mathbb{N},$$

where each node state n_i is

$$n_i = \begin{cases} 0, & \text{free,} \\ \neq 0 & \text{occupied or undetermined.} \end{cases}$$

We denote the set of edges for the undirected graph G as

$$E \triangleq \{c_{ij} \mid i, j \in N\},$$

where c_{ij} denotes the cost of the directed edge from i to j and, since the graph is undirected,

$$c_{ij} = c_{ji}, \quad c_{ij} > 0.$$

We assume there exists a constant $\delta > 0$ such that

$$c_{ij} \geq \delta \quad \forall (i, j) \in E.$$

Let $\Gamma : N \rightarrow \Gamma(N)$ be the successor mapping, where $\Gamma(N)$ denotes the set of neighbors of a node. We denote the starting node and the preferred goal node by $s \in N$ and $t \in N$ respectively. Let the cost functions be

$$g(n) : \mathbb{R}^n \rightarrow \mathbb{R}_+ : \text{Cost from node } s \text{ to node } n, \quad h(n) : \mathbb{R}^n \rightarrow \mathbb{R}_+ : \text{Cost from node } n \text{ to node } t,$$

and the evaluation function

$$f(n) \triangleq g(n) + h(n),$$

which is to be minimized.

The objective of the planner is to find a sequence of nodes.

$$\pi = (n_0, n_1, \dots, n_L), \quad n_0 = s, \quad n_L = t,$$

such that each consecutive pair satisfies $(n_k, n_{k+1}) \in E$, and the total accumulated path cost

$$J(\pi) = \sum_{k=0}^{L-1} c_{n_k n_{k+1}},$$

is minimized. The evaluation function provides an estimate of the total path cost through n and determines the node-expansion order during the search.

For any node n , the successor set $\Gamma(n) \subseteq N$ denotes the set of nodes reachable from n via feasible edges. In grid-based planning, this typically corresponds to the set of adjacent lattice cells (e.g., 4, 8, or 26-connected neighborhoods), whereas in arbitrary graphs it denotes the immediate neighbors with finite edge costs.

From Hart et al. (1968), we additionally define the optimal cost-to-go function,

$$h^*(n) = \min_{\pi:n \rightarrow t} J(\pi),$$

which represents the true minimal cost from n to the goal node t . A heuristic $h(n)$ is called *admissible* if

$$0 \leq h(n) \leq h^*(n), \quad \forall n \in N,$$

and *consistent* if it satisfies

$$h(n) \leq c_{nn'} + h(n'), \quad \forall n' \in \Gamma(n).$$

Finally, the search process maintains an OPEN set of frontier nodes ordered by increasing f -value and a CLOSED set of expanded nodes. At each iteration, the node with minimal $f(n)$ is selected for expansion. The process terminates either when the goal node t is extracted from OPEN or when OPEN becomes empty, in which case no feasible path exists. In the rest of the paper, optimality is measured by path length, while safety is measured by minimum clearance.

3. Unified Path Planner (UPP)

The Unified Path Planner (UPP) is a graph search algorithm that generates safe, efficient, and smooth paths by combining geometric distance cues with a locally computed obstacle-proximity field. Unlike planners that rely on fixed, manually tuned heuristic weights, UPP incorporates an adaptive mechanism that continuously adjusts its heuristic parameters based on real-time feedback during the search.

The UPP employs a heuristic that combines geometric distance-to-go with a locally computed safety potential, enabling the planner to simultaneously account for path efficiency and obstacle avoidance. For any node $n \in N$, the heuristic is defined as

$$h(n) = \alpha l_1(n, t) + (1 - \alpha) l_\infty(n, t) + \beta S(n), \tag{1}$$

where $\alpha \in [0, 1]$ and $\beta > 0$ are adaptive weighting parameters. The terms l_1 and l_∞ correspond to the Manhattan and Chebyshev distances. $l_1(n, t) = \|n - t\|_1$ and $l_\infty(n, t) = \|n - t\|_\infty$.

The choice of combining the Manhattan and Chebyshev distances is motivated by their distinct geometric structures. The level sets of the Chebyshev distance form diamond-shaped contours aligned with the grid axes, encouraging diagonal progression when minimizing cost. In contrast, the level sets of the Manhattan distance form axis-aligned squares, which promote straight-line motion along the horizontal and vertical directions. As illustrated in Fig. 1,

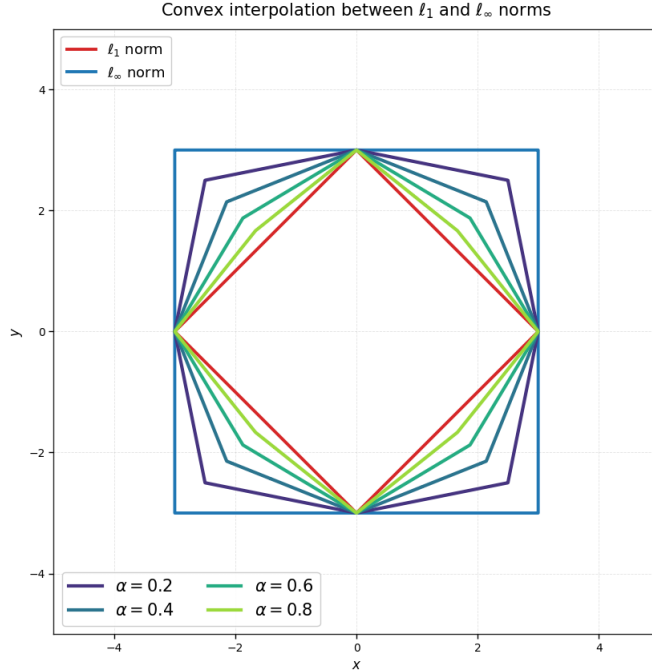


Figure 1: Level set visualization of the ℓ_1 norm , the ℓ_∞ norm , and their convex combinations for multiple values of α .

the color-coded level sets reveal that the combined heuristic inherits desirable properties from both norms, enabling smoother, more natural directional transitions during planning.

The term $S(n)$ represents a safety potential encoding the proximity of node n to surrounding obstacles. It is defined over a Chebyshev-radius neighborhood of size r as

$$S(n) = \sum_{\Delta \in [-r, r]} \frac{\mathbf{1}_{\mathcal{O}}(n + \Delta)}{\|\Delta\|_\infty + \varepsilon}, \quad (2)$$

where $\mathbf{1}_{\mathcal{O}}(n + \Delta)$ is the indicator function, equal to 1 if the grid cell at $n + \Delta$ is occupied by an obstacle and 0 otherwise, $\mathcal{O} \subset N$ denotes the set of obstacle nodes, and $\varepsilon > 0$ prevents division singularity. This formulation implements an inverse-distance accumulation as nearby obstacles contribute larger penalties, while distant obstacles within the safety horizon make smaller contributions. The safety field is efficiently computed via convolution using a preconstructed kernel

$$K(\Delta) = \begin{cases} \frac{1}{\|\Delta\|_\infty + \varepsilon}, & 1 \leq \|\Delta\|_\infty \leq r, \\ 0, & \text{otherwise,} \end{cases}$$

ensuring that $S(n)$ is available in constant time during the search. The safety heuristic for a small grid for $r = 6$ is illustrated in Figure 2

Unlike classical inflation-based heuristics that uniformly pad obstacle regions, the inverse distance safety potential offers a continuous and geometry-aware measure of local risk. This enables the planner to adapt its behavior seamlessly between open, low-risk areas and narrow, obstacle-dense corridors.

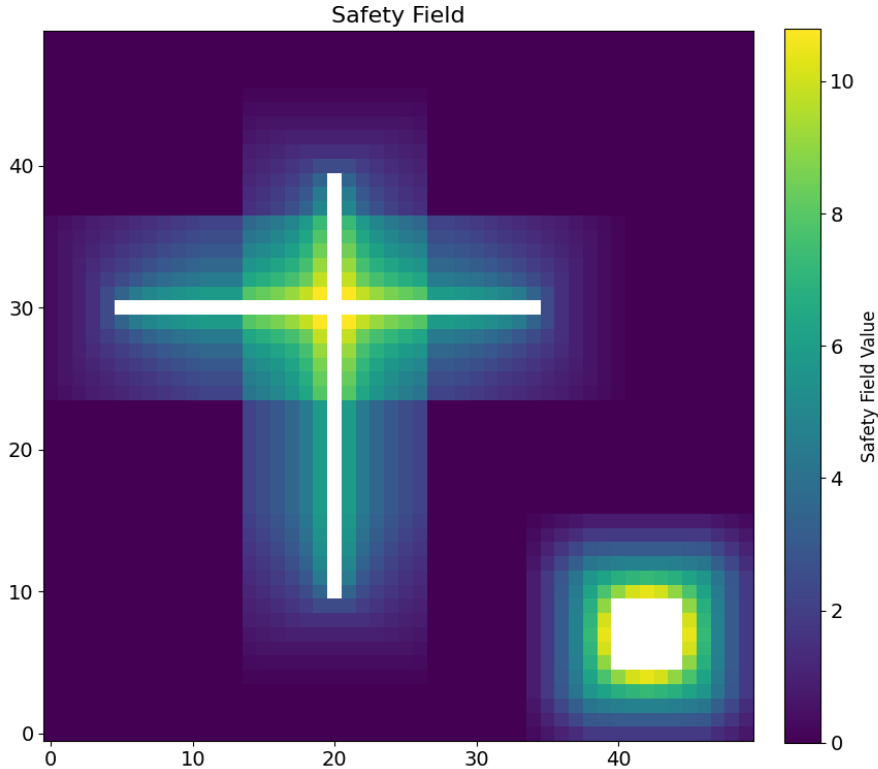


Figure 2: Safety Field on a grid, white area represents obstacles

3.1. Initial Parameter Selection

The Unified Path Planner uses four main heuristic parameters: the distance-mixing weight α , the safety weight β , the safety radius r , and a small constant ε used for numerical stability.

Initially, the distance-mixing weight α is set to $\alpha = 0.5$, which gives an equal balance between the Manhattan and Chebyshev distance terms in the heuristic. This neutral choice avoids biasing the planner toward either purely axis-aligned or purely diagonal motion at the outset. During the search, α is adapted based on the accumulated turning behavior of the path.

The constant $\varepsilon > 0$ appears in the inverse distance safety field to prevent division by zero when an obstacle lies directly adjacent to a node. In practice, a small value such as $\varepsilon = 0.01$ is sufficient to regularize the safety term without noticeably affecting its magnitude.

The initial safety weight β and safety radius R are computed from the geometry of the occupancy grid. Let $D = \text{DT}(G)$ denote the Euclidean distance transform of the free space, computed as

$$D(x) = \text{dist}(x, \mathcal{O}), \quad \mathcal{O} = \{x \mid G(x) = 1\},$$

and let $\mathcal{F} = \{x \mid G(x) = 0\}$ be the set of free cells. We define

$$\mu = \mathbb{E}[D(x) \mid x \in \mathcal{F}], \quad \sigma = \text{Std}[D(x) \mid x \in \mathcal{F}],$$

as the mean and standard deviation of the free space distance field, and

$$\rho = \frac{|\mathcal{O}|}{|G|}$$

as the obstacle density, i.e., the fraction of occupied cells in the grid. Intuitively, larger ρ and larger relative variability $\sigma/(\mu + \varepsilon)$ indicates more cluttered or irregular environments, in which safety should be weighted more strongly.

Given a user-specified base value β , the initial safety weight is scaled according to

$$\beta_{\text{init}} = \text{clip}\left(\frac{\beta\rho\sigma}{\mu + \varepsilon}, \beta_{\text{min}}, \beta_{\text{max}}\right), \quad (3)$$

where $\text{clip}(\cdot, \beta_{\text{min}}, \beta_{\text{max}})$ saturates the value to lie within predefined bounds $[\beta_{\text{min}}, \beta_{\text{max}}]$. This mapping increases β in dense, highly variable environments and attenuates it in sparse, more uniform maps, thereby adapting the safety influence to the overall structure of the workspace.

Similarly, the initial safety radius R is rescaled using the same statistics:

$$r_{\text{init}} = \text{clip}(\text{round}(r(\mu + \sigma)), r_{\text{min}}, r_{\text{max}}), \quad (4)$$

Larger values of $\mu + \sigma$ typically correspond to more spacious environments, for which a larger lookahead radius is beneficial, whereas tighter or more cluttered maps keep r small to control computational cost.

3.2. Adaptation of Parameters

UPP incorporates online parameter adaptation for both the safety weight β and the distance mixing parameter α , enabling the heuristic to respond dynamically to local geometry and search progress. These updates operate after the geometry-aware initialization described in Algorithm 1 and are applied during node expansion.

Let n_i denote the node expanded at iteration i , and let

$$d_i \triangleq \|n_i - t\|_2$$

be its Euclidean distance to the goal. We define the signed progress.

$$\Delta d_i \triangleq d_i - d_{i-1}.$$

Given a tolerance $\tau_{\text{goal}} > 0$, we define a progress indicator

$$p_i = \begin{cases} +1, & \Delta d_i < -\tau_{\text{goal}} \quad , \text{ progress} \\ -1, & \Delta d_i > \tau_{\text{goal}} \quad , \text{ regression} \\ 0, & |\Delta d_i| \leq \tau_{\text{goal}} \quad , \text{ stall.} \end{cases}$$

A stall counter s_i is maintained as

$$s_i = \begin{cases} 0, & p_i \neq 0, \\ s_{i-1} + 1, & p_i = 0. \end{cases}$$

Let $\gamma_{\text{rec}} > 1$ and $\gamma_{\text{dec}} \in (0, 1)$ denote multiplicative recovery and decay factors, and let $[\beta_{\min}, \beta_{\max}]$ be fixed bounds. The safety weight is updated according to

$$\beta_{i+1} = \Pi_{[\beta_{\min}, \beta_{\max}]} \left(\beta_i \gamma_{\text{rec}}^{\mathbf{1}_{\{p_i=+1\}}} \gamma_{\text{dec}}^{\mathbf{1}_{\{p_i=-1\}} + \mathbf{1}_{\{s_i \geq K_\beta\}}} \right). \quad (5)$$

where $\Pi_{[a,b]}(\cdot)$ denotes projection onto $[a, b]$, $\mathbf{1}_A$ is the indicator function in set A , and K_β is a patience threshold. This rule reduces β when the search stalls or moves away from the goal, allowing escape from overly conservative regions, while increasing β during sustained progress to encourage safer exploration.

To regulate path smoothness, UPP adapts the distance mixing parameter α based on turning behavior. Let $p(n_i)$ denote the parent of n_i , and define the motion and goal direction vectors

$$v_i = n_i - p(n_i), \quad g_i = t - n_i.$$

Let θ_i^{move} and θ_i^{goal} be their headings, and define the wrapped angular deviation

$$\theta_i \triangleq \left| \text{wrap}_{[-\pi, \pi]} \left(\theta_i^{\text{goal}} - \theta_i^{\text{move}} \right) \right|.$$

where $\text{wrap}_{[-\pi, \pi]}(\alpha) \triangleq ((\alpha + \pi) \bmod 2\pi) - \pi$.

Over a window of length K_α , UPP accumulates deviation relative to a target turning angle θ_{tar} :

$$u_i \triangleq \sum_{j=i-K_\alpha+1}^i (\theta_j - \theta_{\text{tar}}).$$

With hysteresis threshold $\tau_{\text{ang}} > 0$, recovery factor $\eta_{\text{rec}} > 1$, decay factor $\eta_{\text{dec}} \in (0, 1)$, and bounds $[\alpha_{\min}, \alpha_{\max}]$, the update rule is

$$\alpha_{i+1} = \begin{cases} \Pi_{[\alpha_{\min}, \alpha_{\max}]}(\alpha_i \eta_{\text{rec}}), & u_i > \tau_{\text{ang}}, \\ \Pi_{[\alpha_{\min}, \alpha_{\max}]}(\alpha_i \eta_{\text{dec}}), & u_i < -\tau_{\text{ang}}, \\ \alpha_i, & \text{otherwise.} \end{cases} \quad (6)$$

Increasing α strengthens the Manhattan component of the hybrid distance, discouraging diagonal motion, while decreasing α permits greater diagonal freedom via the Chebyshev component.

Global map statistics provide a well-scaled prior, while online adaptivity balances safety, optimality, and smoothness as the search evolves.

3.3. Theoretical Properties

3.3.1. Completeness of UPP

Lemma 1. *Provided the parameters $\alpha \in (0, 1)$ and $\beta \in [\beta_{\min}, \beta_{\max}]$ are updated according to the update laws (6) and (5) respectively, then the heuristic function $h(\cdot)$ is bounded by*

$$h(n) \leq h^*(n) + \beta_{\max} \sum_{d=1}^r \frac{(2d+1)^n - (2d-1)^n}{d + \varepsilon}, \quad (7)$$

where n denotes the dimension of the grid, r denotes the distance at which the neighbors are considered, $\varepsilon \in \mathbb{R}$ is the parameter defined in (2)

Proof. The planner is initialized with user-specified base parameters (α_0, β_0, R_0) . Before planning, β and R are rescaled using statistics of the distance transform of free space and then clipped to fixed compact intervals $[\beta_{\min}, \beta_{\max}]$ and $[R_{\min}, R_{\max}]$. The mixing parameter α is similarly restricted to a compact interval $[\alpha_{\min}, \alpha_{\max}] \subset (0, 1)$.

During the search, β is updated multiplicatively based on signed progress towards the goal, and α is also updated multiplicatively based on accumulated turn demand over a sliding window. Both parameters are projected within limits. So,

$$\alpha_{\min} \leq \alpha \leq \alpha_{\max}, \quad \beta_{\min} \leq \beta \leq \beta_{\max}.$$

The safety field S is computed by convolving the binary obstacle indicator with a kernel of finite support (radius $r \in [r_{\min}, r_{\max}]$) and bounded magnitude. Since the grid and kernel support are finite and the kernel entries are uniformly bounded, there exists $S_{\max} < \infty$ such that

$$0 \leq S(n) \leq S_{\max} \quad \text{for all } n.$$

A node that is completely surrounded by obstacles (i.e. all neighbours satisfy $\|m - n\|_{\infty} = 0$) is never explored by the planner. Therefore, for every *explored* node n , all contributing obstacle cells satisfy the lower bound

$$\|m - n\|_{\infty} \geq d.$$

for a distance d from the cell. As for the cell to be explored, it must have one direction of free grid cells. To obtain a worst-case bound on $S(n)$, we count the number of obstacle cells that can lie at each Chebyshev distance d from n . In an n -dimensional grid, the number of grid cells at *exact* Chebyshev distance d is

$$k_d = (2d + 1)^n - (2d - 1)^n.$$

These correspond to the shell between hypercubes of radius d and $d - 1$.

The contribution of each such cell is at most $1/(d + \varepsilon)$. Hence, the maximum possible safety value at any explored node is

$$S_{\max} = \sum_{d=1}^r \frac{k_d}{d + \varepsilon} = \sum_{d=1}^r \frac{(2d + 1)^n - (2d - 1)^n}{d + \varepsilon}.$$

This expression provides a tight worst-case upper bound for the proposed inverse-distance safety field in n dimensions.

$$l_1(n, t) \leq h^*(n), \quad l_{\infty}(n, t) \leq h^*(n) \quad \text{for all } n.$$

Hence, at any node n it can be written as,

$$\begin{aligned} h(n) &= \alpha l_1(n, t) + (1 - \alpha) l_{\infty}(n, t) + \beta S(n) \\ &\leq \alpha h^*(n) + (1 - \alpha) h^*(n) + \beta_{\max} \sum_{d=1}^r \frac{(2d + 1)^n - (2d - 1)^n}{d + \varepsilon} \\ &\leq h^*(n) + \beta_{\max} \sum_{d=1}^r \frac{(2d + 1)^n - (2d - 1)^n}{d + \varepsilon} \end{aligned}$$

The constant $h^*(n)$ depends only on the grid size and the fixed parameter ranges, not on the particular adaptive trajectory of (α, β) . Thus the heuristic remains uniformly bounded throughout the search. \square

Remark. This bound provides a worst-case performance guarantee for UPP. In practice, the proximity penalty rarely saturates to its maximum over every step, so observed path costs are typically much closer to the optimal cost.

Lemma 2. *Let n be the currently expanded node and let $m_i, m_j \in \mathcal{N}(n)$ be two neighbors. Suppose the UPP heuristic is*

$$h(m) = d(m, t) + \beta S(m),$$

where $d(\cdot, t)$ is the distance heuristic and $S(\cdot)$ is the safety score, bounded as $0 \leq S(m) \leq S_{\max}$.

If

$$|d(m_i, t) - d(m_j, t)| \leq c \quad \text{and} \quad \beta|S(m_i) - S(m_j)| > c,$$

then

$$h(m_i) < h(m_j) \iff S(m_i) > S(m_j).$$

In particular, when the current node is sufficiently far from the goal so that distance variations among neighbors are bounded by c , the heuristic ordering is dominated by safety differences.

Proof. For any two neighbors m_i, m_j of n , the heuristic difference satisfies

$$h(m_i) - h(m_j) = [d(m_i, t) - d(m_j, t)] + \beta[S(m_i) - S(m_j)].$$

When n is far from the goal, the grid structure implies that the one-step distance variations are bounded, i.e.,

$$|d(m_i, t) - d(m_j, t)| \leq c,$$

for some constant $c > 0$.

If $\beta|S(m_i) - S(m_j)| > c$, the safety term strictly dominates the distance term, and therefore the sign of $h(m_i) - h(m_j)$ is determined by $S(m_i) - S(m_j)$. Hence,

$$h(m_i) < h(m_j) \iff S(m_i) > S(m_j),$$

so the neighbor with higher safety is preferred.

As n approaches the goal, the variation in $d(\cdot, t)$ among neighbors becomes comparable to or larger than the safety variation, and the distance term governs the ordering. Thus, UPP prioritizes safety when safety differences are meaningful, and reverts to distance-based ordering near the goal. \square

Theorem 1. *If a collision-free path from s to t exists in G , then UPP terminates with success and returns a valid suboptimal path while favoring safety. Otherwise, it correctly reports failure.*

Proof. As the heuristics cost is bounded according to Lemma 1, the queue insertions and reinsertions (due to the minimum heap) would be finite. This leads to two possible termination cases.

Case (i): The goal t is popped from the queue. Then $t \neq s$ must have been discovered from a neighbor n and assigned $\text{parent}(t) = n$. Recursively following parent pointers decreases g monotonically and must reach s in finitely many steps, yielding a valid path prioritizing safety (Lemma 2)).

Case (ii): The queue becomes empty without expanding t . Then all free states reachable from s have been expanded or found not to improve the cost. Hence, t is unreachable via free states and no collision-free path exists.

In both cases the returned result is correct. Thus, UPP is complete. \square

3.3.2. Effect of adaptive β

We analyze how the adaptive safety weight β affects the heuristic values along the path and consequently influences both suboptimality and safety. For any node n with goal t , the heuristic is

$$h^{(\beta)}(n, t) = d(n, t) + \beta S(n), \quad (8)$$

where $d(n, t)$ is the geometric distance term and $S(n)$ is the proximity-based safety cost. Assume the successors $k_i, i = 1, 2, \dots, b$ are elements of the current OPEN set during expansion, and are from almost equal distances away from the goal.

Consider two safety weights β_o (old) and β_n (new). For any forward neighbor k_{b+i} , the change in heuristic becomes

$$\delta h = h^{(\beta_n)}(k_{b+i}) - h^{(\beta_o)}(k_{b+i}) = (\beta_n - \beta_o) S(k_{b+i}). \quad (9)$$

On decreasing β , $\beta_n < \beta_o$, then from (9) we have

$$\delta h = (\beta_n - \beta_o) S(k_{b+i}) < 0,$$

because $S(k_{l+i}) \geq 0$. Thus, the heuristic systematically decreases at every successor node:

$$h^{(\beta_n)}(k_{l+i}) < h^{(\beta_o)}(k_{l+i}). \quad (10)$$

Substituting this decrease into the standard A* inequality,

$$d(m, t) + \beta_o S(m) \leq h^*(m, t) + \Delta,$$

on given Δ represents the average suboptimality bound due to the average safety cost term, and using $-\delta h > 0$. Adding δh on both sides

$$d(n, t) + \beta_o S(n) + \delta h \leq h^*(n, t) + \Delta + \delta h. \quad (11)$$

$$d(n, t) + \beta_n S(n) \leq h^*(n, t) + \Delta + \delta h. \quad (12)$$

Since $-\delta h > 0$, the suboptimality bound decreases by δh which leads to improved cost for suboptimality

While on increasing β , safety weight increases preferring safer nodes for further planning according to lemma 2.

3.3.3. Effect of adaptive α

On the given distance heuristic assuming constant safety,

$$d(n, t) = \alpha(t) l_1(n, t) + (1 - \alpha(t)) l_\infty(n, t). \quad (13)$$

After the adaptive update α changed to α_c the change in the heuristic is

$$\Delta d(n, t) = d^{(\alpha_c)}(n, t) - d^{(\alpha)}(n, t) \quad (14)$$

$$= \alpha_c l_1(n, t) + (1 - \alpha_c) l_\infty(n, t) - [\alpha l_1(n, t) + (1 - \alpha) l_\infty(n, t)] \quad (15)$$

$$= (\alpha_c - \alpha) (l_1(n, t) - l_\infty(n, t)) \quad (16)$$

$$= \delta\alpha (l_1(n, t) - l_\infty(n, t)). \quad (17)$$

For $\delta\alpha = \alpha_c - \alpha$

Since on grid maps $l_1(n, t) > l_\infty(n, t)$, the sign of $\Delta d(n, t)$ is determined entirely by the sign of $\delta\alpha$:

- $\delta\alpha > 0$: Since $l_1(n, t) > l_\infty(n, t)$, we obtain $\Delta d(n, t) > 0$. The Manhattan component gains weight, increasing the cost of lateral or diagonal deviation. Hence the heuristic favours grid-aligned, goal-directed motion, reinforcing a correct heading.
- $\delta\alpha < 0$: Then $\Delta d(n, t) < 0$, reducing the influence of l_1 and making the heuristic more Chebyshev-like. This lowers directional bias and permits diagonal, exploratory adjustments, which is useful when the current motion is ineffective or moving away from the goal.

As the sign of $\Delta d(n, t)$ matches the sign of $\delta\alpha$, adaptive α acts as a direction-aware shaping term: progress toward the goal strengthens commitment to the current direction, while the regressor reduces this commitment and promotes reorientation. This establishes a self-correcting directional mechanism that improves convergence and avoids persistent deviation from the goal.

3.4. Algorithm

The pseudo-algorithm for the UPP main search is presented in Algorithm 3. UPP computes a path over a grid from a given start to a given goal using adaptive heuristic components. The process begins with the geometry-aware initialization of parameters, described in Algorithm 1. Here, the safety weight β is initialized based on obstacle density and spatial variability, while the radius R is scaled according to the proximity of obstacles, providing an estimate of how much local risk needs to be evaluated. The safety field is computed as an inverse-distance accumulation over a Chebyshev neighborhood at this stage and serves as a safety-aware heuristic term.

During the graph search in Algorithm 3, the UPP continuously adapts its heuristic parameters using the update rules in Algorithm 2. The safety parameter β is adjusted through stall detection when the search fails to progress meaningfully toward the goal, while the distance mixing parameter α is updated based on directional alignment with the goal. These adaptive updates enable UPP to dynamically balance optimality, safety, and smoothness throughout the planning process.

Algorithm 1: INITUPP: Geometry Aware Initialization

Input: Occupancy grid G ; base $(\alpha_{\text{base}}, \beta_{\text{base}}, R_{\text{base}}, \varepsilon)$

Input: Bounds $(\beta_{\text{min}}, \beta_{\text{max}}, R_{\text{min}}, R_{\text{max}})$

Output: Initialized α, β, R and safety field $S(\cdot)$

$\alpha \leftarrow \alpha_{\text{base}}; \quad \beta \leftarrow \beta_{\text{base}}; \quad R \leftarrow R_{\text{base}};$

Compute Euclidean distance transform D over free cells of G ;

$\mathcal{F} \leftarrow \{x \mid G(x) = 0\}; \quad \mathcal{O} \leftarrow \{x \mid G(x) = 1\};$

$\mu \leftarrow \text{mean}(D(x) \mid x \in \mathcal{F}); \quad \sigma \leftarrow \text{std}(D(x) \mid x \in \mathcal{F}); \quad \rho \leftarrow \frac{|\mathcal{O}|}{|\mathcal{F}|};$

$\beta \leftarrow \text{clip}\left(\beta \rho \frac{\sigma}{\mu + \varepsilon}, \beta_{\text{min}}, \beta_{\text{max}}\right);$

$R \leftarrow \text{clip}(\text{round}(R(\mu + \sigma)), R_{\text{min}}, R_{\text{max}});$

Build Chebyshev kernel $K(\Delta) = 1/(\|\Delta\|_{\infty} + \varepsilon)$ for $1 \leq \|\Delta\|_{\infty} \leq R$, else 0;

Convolve obstacle grid with K to obtain S_{sum} ;

Set $S(x) \leftarrow S_{\text{sum}}(x)$ for free cells, 0 for obstacles;

return $(\alpha, \beta, R, S(\cdot));$

4. OptiSafe Index

This section introduces the *OptiSafe* index, a normalized metric designed to evaluate planning algorithms by jointly considering *optimality* and *safety*. Unlike metrics that assess these dimensions separately, the OptiSafe index penalizes imbalance towards one metric and rewards equal uplift.

Consider a path planning algorithm P given a start position s and an end goal t . We denote the path length of P by $L(P)$. Correspondingly, we denote the optimal path length by $L(\text{optimal})$.

The deviation from optimality is defined as

$$O_D = \min\left(1, \max\left(0, \frac{L(P) - L(\text{optimal})}{L(\text{optimal})}\right)\right).$$

The *optimality index* is defined as

$$O(P) = 1 - O_D,$$

which ensures $O(P) \in [0, 1]$.

Additionally, we define the minimum clearance of the planner P from the obstacles as $D(P)$. Consider a path planning algorithm that doesn't prioritize optimality but is tasked only with keeping the planner safe. The minimum clearance of the safe planner is denoted as $D(\text{safe})$.

Define the *safety deviation* as

$$C_D = \begin{cases} 0, & \text{if } D(P) \geq D(\text{safe}), \\ \frac{D(\text{safe}) - D(P)}{D(\text{safe})}, & \text{otherwise.} \end{cases}$$

The *safety index* is

$$C(P) = 1 - C_D,$$

Algorithm 2: UPDATEPARAMS: Adaptive Update of β and α

Input: Current node n , goal t , parent map $\text{parent}(\cdot)$
Input: Current α, β , and state: $\text{prev_dist}, \text{stalled}, \text{turn_sum}, \text{turn_iter}$
Input: Hyperparameters for β : $\tau_{\text{goal}}, K_{\beta}, \beta_{\text{min}}, \beta_{\text{max}}, \gamma_{\text{dec}}, \gamma_{\text{rec}}$
Input: Hyperparameters for α : $\tau_{\text{ang}}, K_{\alpha}, \alpha_{\text{min}}, \alpha_{\text{max}}, \eta_{\text{dec}}, \eta_{\text{rec}}, \theta_{\text{tar}}$
Output: Updated α, β and state variables

$\text{cur_dist} \leftarrow \|n - t\|_2; \quad \Delta d \leftarrow \text{cur_dist} - \text{prev_dist};$
if $\Delta d < -\tau_{\text{goal}}$ **then**
 $\text{stalled} \leftarrow 0; \quad \beta \leftarrow \min(\beta \cdot \gamma_{\text{rec}}, \beta_{\text{max}});$
else if $\Delta d > \tau_{\text{goal}}$ **then**
 $\text{stalled} \leftarrow 0; \quad \beta \leftarrow \max(\beta \cdot \gamma_{\text{dec}}, \beta_{\text{min}});$
else
 $\text{stalled} \leftarrow \text{stalled} + 1;$
 if $\text{stalled} \geq K_{\beta}$ **then**
 $\beta \leftarrow \max(\beta \cdot \gamma_{\text{dec}}, \beta_{\text{min}}); \quad \text{stalled} \leftarrow 0;$
 $\text{prev_dist} \leftarrow \text{cur_dist};$
if $\text{parent}(n)$ *defined* **then**
 $p \leftarrow \text{parent}(n);$
 $\mathbf{v}_{\text{move}} \leftarrow n - p; \quad \mathbf{v}_{\text{goal}} \leftarrow t - n;$
 Compute $\theta_{\text{move}}, \theta_{\text{goal}}; \quad \theta_{\text{raw}} \leftarrow \text{wrap}_{[-\pi, \pi]}(\theta_{\text{goal}} - \theta_{\text{move}});$
 $\theta_{\text{turn}} \leftarrow |\theta_{\text{raw}}|;$
else
 $\theta_{\text{turn}} \leftarrow 0;$
 $\text{turn_sum} \leftarrow \text{turn_sum} + (\theta_{\text{turn}} - \theta_{\text{tar}});$
 $\text{turn_iter} \leftarrow \text{turn_iter} + 1;$
if $\text{turn_iter} \geq K_{\alpha}$ **then**
 if $\text{turn_sum} > \tau_{\text{ang}}$ **then**
 $\alpha \leftarrow \min(\alpha \cdot \eta_{\text{rec}}, \alpha_{\text{max}});$
 else if $\text{turn_sum} < -\tau_{\text{ang}}$ **then**
 $\alpha \leftarrow \max(\alpha \cdot \eta_{\text{dec}}, \alpha_{\text{min}});$
 $\text{turn_sum} \leftarrow 0; \quad \text{turn_iter} \leftarrow 0;$
return $(\alpha, \beta, \text{prev_dist}, \text{stalled}, \text{turn_sum}, \text{turn_iter});$

Algorithm 3: Unified Path Planner (UPP): Main Search

Input: Occupancy grid G , start node s , goal node t

Input: Parameters:

$\{\alpha_{\text{base}}, \beta_{\text{base}}, R_{\text{base}}, \varepsilon, \beta_{\text{min}}, \beta_{\text{max}}, \gamma_{\text{dec}}, \gamma_{\text{rec}}, K_{\beta}, \tau_{\text{goal}}, \alpha_{\text{min}}, \alpha_{\text{max}}, \eta_{\text{dec}}, \eta_{\text{rec}}, \tau_{\text{ang}}, \theta_{\text{tar}}, K_{\alpha}, R_{\text{min}}, R_{\text{max}}\}$

Output: Path π from s to t if found; failure otherwise

if s or t invalid or occupied in G **then**

└ **return** failure

if $s = t$ **then**

└ **return** (s)

$(\alpha, \beta, R, S) \leftarrow \text{INITUPP}(G)$;

Initialize $g(n) \leftarrow +\infty$ for all n ; $g(s) \leftarrow 0$;

$V \leftarrow \emptyset$; $\text{parent}(\cdot)$ undefined;

Define $h(n, t) = \alpha \ell_1(n, t) + (1 - \alpha) \ell_{\infty}(n, t) + \beta S(n)$;

Initialize OPEN as priority queue; push $(f(s), g(s), s)$ with $f(s) = g(s) + h(s, t)$;

$\text{prev_dist} \leftarrow \|s - t\|_2$; $\text{stalled} \leftarrow 0$; $\text{turn_sum} \leftarrow 0$; $\text{turn_iter} \leftarrow 0$;

while OPEN not empty **do**

┌ Pop (f, g, n) with smallest f from OPEN;

┌ **if** $n \in V$ **then**

└ **continue**

┌ Add n to V ;

┌ **if** $n = t$ **then**

└ **goto** PathReconstruction

┌ $(\alpha, \beta, \text{prev_dist}, \text{stalled}, \text{turn_sum}, \text{turn_iter}) \leftarrow$

┌ UPDATEPARAMS($n, t, \text{parent}, \alpha, \beta, \text{prev_dist}, \text{stalled}, \text{turn_sum}, \text{turn_iter}$);

┌ **foreach** neighbor $m \in \Gamma(n)$ **do**

└ **if** m invalid, occupied, or $m \in V$ **then**

└└ **continue**

└ Compute step cost c_{nm} ;

└ $g_{\text{new}} \leftarrow g + c_{nm}$;

└ **if** $g_{\text{new}} < g(m)$ **then**

└└ $g(m) \leftarrow g_{\text{new}}$; $\text{parent}(m) \leftarrow n$;

└└ $f(m) \leftarrow g(m) + h(m, t)$;

└└ Push $(f(m), g(m), m)$ into OPEN;

PathReconstruction;

if $n \neq t$ **then**

└ **return** failure

Initialize empty path π ;

while n defined **do**

└ Prepend n to π ; $n \leftarrow \text{parent}(n)$;

return π ;

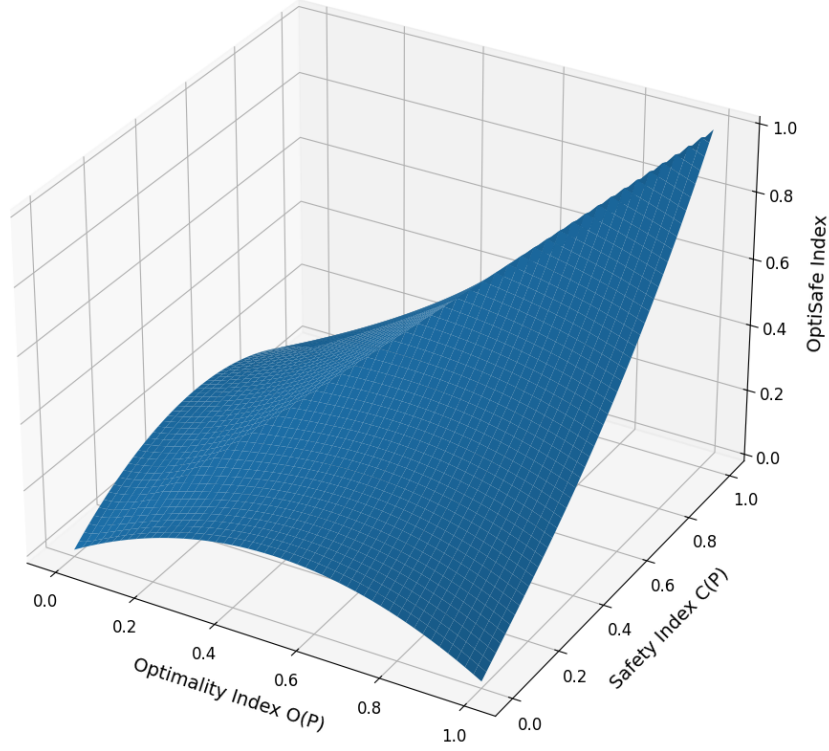


Figure 3: Optisafe Index Surface

which also lies in $[0, 1]$.

We combine the two into a balanced measure:

$$\text{OptiSafe}(P) = \left(1 - |O(P) - C(P)|\right) \frac{\sqrt{O(P)^2 + C(P)^2}}{\sqrt{2}}. \quad (18)$$

For simplicity, set $O := O(P)$, $C := C(P)$. Then

$$B(O, C) = 1 - |O - C| \quad , \text{ balance term}$$

$$R(O, C) = \frac{\sqrt{O^2 + C^2}}{\sqrt{2}} \quad , \text{ strength term.}$$

An illustration of the Optisafe Index surface as a function of the optimality and safety indices is shown in Fig. 3.

4.1. Theoretical properties

Lemma 3. For all planners P , $0 \leq O(P) \leq 1$ and $0 \leq C(P) \leq 1$

Proof. By construction, $O_D = \min(1, \max(0, x))$ with $x = \frac{L(P) - L(\text{optimal})}{L(\text{optimal})}$. Thus $0 \leq O_D \leq 1$. Since $O(P) = 1 - O_D$, we have $0 \leq O(P) \leq 1$. Further for $C(P)$,

Case 1: If $D(P) \geq D(\text{safe})$, then $C_D = 0$ and $C(P) = 1$. Case 2: If $D(P) < D(\text{safe})$, then $0 \leq (D(\text{safe}) - D(P))/D(\text{safe}) \leq 1$. Hence $0 \leq C_D \leq 1$, and $C(P) = 1 - C_D \in [0, 1]$. \square

Lemma 4. Considering $O(P)$ and $C(P)$ to be O and C respectively. As $O, C \in [0, 1]$. Define

$$B(O, C) = 1 - |O - C|, \quad R(O, C) = \frac{\sqrt{O^2 + C^2}}{\sqrt{2}}.$$

Then the following hold:

1. $0 \leq B(O, C) \leq 1$ and $0 \leq R(O, C) \leq 1$.
2. $B(O, C) = 1$ if and only if $O = C$, and $B(O, C) = 0$ if and only if $|O - C| = 1$.
3. $R(O, C) = 1$ if and only if $O = C = 1$, and $R(O, C) = 0$ if and only if $O = C = 0$.

Proof. Since $O, C \in [0, 1]$, it follows that $|O - C| \in [0, 1]$, and hence

$$0 \leq B(O, C) = 1 - |O - C| \leq 1.$$

The equality cases follow directly from properties of the absolute value.

Moreover, $0 \leq O^2 + C^2 \leq 2$, which implies

$$0 \leq R(O, C) = \frac{\sqrt{O^2 + C^2}}{\sqrt{2}} \leq 1.$$

The upper bound is achieved if and only if $O^2 + C^2 = 2$, i.e., $O = C = 1$, while the lower bound holds if and only if $O = C = 0$. \square

Theorem 2. For all $O, C \in [0, 1]$,

1. $0 \leq \text{OptiSafe}(O, C) \leq 1$.
2. $\text{OptiSafe}(O, C) = \text{OptiSafe}(C, O)$.

Proof. (i) From lemma 4, $B \in [0, 1]$ and $R \in [0, 1]$. Their product lies in $[0, 1]$. upper bound 1 is achieved at $O = C = 1$, lower bound 0 occurs if $O = C = 0$ or $|O - C| = 1$.

(ii) Both components are symmetric: $|O - C| = |C - O|$, and $O^2 + C^2 = C^2 + O^2$. \square

Remark: OptiSafe enforces *conditional monotonicity*, rewarding equal uplift and penalizing imbalance. This design ensures that planners are evaluated not only for strength but also for harmony between optimality and safety.

4.2. Algorithm

Algorithm 4: OptiSafe Index Evaluation

Input: Start state s , goal state t , grid map G , cell size c , planner path P

Output: OptiSafe Index \mathcal{O}

$P_{optimal} \leftarrow \text{OptimalPlanner.plan}(s, g, M)$

$L(\text{Optimal}) \leftarrow \text{PathCost}(P_{optimal}, c)$

$L(P) \leftarrow \text{PathCost}(P, c)$

$P_{safe} \leftarrow \text{HighSafetyPlanner.plan}(s, g, M)$

$D(\text{safe}) \leftarrow \text{MinimumClearance}(P_{safe}, c)$

$D(P) \leftarrow \text{MinimumClearance}(P, c)$

if $D(\text{safe}) > 0$ **then**

if $D(P) > D(\text{safe})$ **then**

$cd \leftarrow 0$

else

$cd \leftarrow \frac{D(\text{safe}) - D(P)}{D(\text{safe})}$

else

$cd \leftarrow 1$

if $L(\text{Optimal}) > 0$ **then**

$od \leftarrow \min\left(1, \max\left(\frac{L(P) - L(\text{Optimal})}{L(\text{Optimal})}, 0\right)\right)$

else

$od \leftarrow 1$

$o \leftarrow 1 - od$

$c \leftarrow 1 - cd$

$\mathcal{OSI} \leftarrow \frac{(1 - |o - c|) \cdot \sqrt{o^2 + c^2}}{\sqrt{2}}$

return \mathcal{OSI}

The pseudo-algorithm for computing the OptiSafe Index is presented in Algorithm 4. For the planner under evaluation, we first obtain its path using its standard planning routine. To normalize safety and optimality, we additionally compute two reference paths: (i) an optimal path, which provides the minimal achievable path length, and (ii) a safe path, which provides the maximal achievable clearance. These reference paths define the lower bound on path cost and the upper bound on safety, respectively. Using these values, the optimality and safety indices are computed as described earlier. Finally, substituting these indices into Eq. 18, the OptiSafe Index is evaluated.

5. Simulation results

5.1. UPP ablation studies

We perform ablation studies for UPP on a 1000×1000 grid with a cell size of 0.05 m. All path lengths (in m) and clearances (in cm) are reported in the world frame with grid size taken into account. Table 1 evaluates the effect of making the parameters α and β adaptive in both a sparse and a cluttered environment. These simulations have been conducted on a 13th Gen Intel(R) Core(TM) i7-13650HX 2.60 GHz processor and 16 GB RAM.

In the sparse environment, using fixed (α, β) requires approximately 2204.69 ms of planning time. Making only α adaptive reduces the planning time to 332.50 ms, reducing it drastically while balancing diagonal and grid-based movements, while keeping the path length essentially unchanged. When only β is adaptive, the planning time remains comparable to the fixed case, but the minimum clearance increases from 0.14 m to 0.25 m, reflecting more conservative, safety-oriented behavior in the low-density setting. When both α and β are adaptive, planning time is further reduced to 267.06 ms and clearance increases to 0.30 m. At the same time, the total turning angle drops from 228.82° to 138.85° , indicating smoother, less zig-zag paths.

A similar pattern is observed in the cluttered environment. With both parameters fixed, UPP requires 8383.19 ms and produces high-angle paths with a total turning angle of 2794.59° . Making only α adaptive reduces planning time to 1381.68 ms and decreases the total turning angle to 769.76° , while keeping path length and clearance essentially unchanged. In contrast, making only β adaptive slightly increases planning time and turning, and does not improve clearance in the cluttered case, as the planner tends to spend more time in high-safety regions and can get stuck in local safe pockets. When both parameters are adaptive, the behavior closely matches the adaptive- α case: planning time is 1431.35 ms and the turning angle is 769.76° , suggesting that adaptivity in α is primarily responsible for the efficiency and smoothness gains in cluttered environments.

Table 1: Effect of adaptive α and β in sparse and cluttered environments.

| Sparse Environment | | | | |
|------------------------------|-----------|------------|----------------|------------|
| Method | Time (ms) | Length (m) | Clearance (cm) | Turn (deg) |
| Both fixed | 2204.69 | 75.27 | 14.21 | 228.82 |
| Adaptive α | 332.50 | 75.30 | 18.54 | 228.82 |
| Adaptive β | 2228.83 | 75.41 | 25.14 | 228.84 |
| Both Adaptive | 267.06 | 75.44 | 30.12 | 138.85 |
| Cluttered Environment | | | | |
| Method | Time (ms) | Length (m) | Clearance (cm) | Turn (deg) |
| Both fixed | 8383.19 | 73.32 | 25.47 | 2794.59 |
| Adaptive α | 1381.68 | 73.50 | 30.32 | 769.76 |
| Adaptive β | 8502.23 | 73.32 | 25.75 | 2884.58 |
| Both Adaptive | 1431.35 | 73.51 | 30.59 | 769.76 |

Table 2 studies the robustness of UPP with fully adaptive parameters to the initialization (α_0, β_0) . We vary (α_0, β_0) over more than one order of magnitude in β_0 , from $(0.25, 2.5)$ to $(0.75, 40)$. Across all tested initializations, path length, clearance, and turning angle are identical (up to numerical rounding) in both sparse and cluttered environments. Planning time varies by at most about 10%. These results indicate that UPP with adaptive parameters is insensitive to the choice of initial (α_0, β_0) and does not require careful tuning.

Table 2: Robustness to initialization of (α_0, β_0) with full adaptivity.

| Sparse Environment | | | | |
|------------------------------|-----------|------------|----------------|------------|
| Init (α_0, β_0) | Time (ms) | Length (m) | Clearance (cm) | Turn (deg) |
| (0.25, 2.5) | 304.67 | 75.44 | 30.13 | 138.85 |
| (0.50, 10) | 271.38 | 75.44 | 30.13 | 138.85 |
| (0.75, 40) | 287.75 | 75.44 | 30.13 | 138.85 |
| Cluttered Environment | | | | |
| Init (α_0, β_0) | Time (ms) | Length (m) | Clearance (cm) | Turn (deg) |
| (0.25, 2.5) | 1440.98 | 73.51 | 30.13 | 769.76 |
| (0.50, 10) | 1405.65 | 73.51 | 30.13 | 769.76 |
| (0.75, 40) | 1466.70 | 73.51 | 30.13 | 769.76 |

5.2. Planners Comparison

The planners have been compared on various metrics such as planning time (Time (ms)), minimum Clearance along the path (Clearance (cm)), turning angle (Turn(deg)), path length (Length(m)) , success rate (SR, in percent) and OptiSafe Index(OSI). The comparison of UPP has been done with A* (Hart et al. (1968)), Voronoi Planner (Ayawli et al. (2019)), RRT (LaValle (2006)), SDF-A* (Wang et al. (2023)), Optimized-A* (Chu et al. (2024)), CBF-RRT (Manjunath and Nguyen (2021)), FS Planner (Cobano et al. (2025)). They have been compared on a 1000 X 1000 grid, with a resolution of 0.05 m for 100 random starts and goals for all environments. Metrics results have been scaled according to the resolution. Planners have been compared in a sparse environment (Table 3) and in a cluttered environment (Table 4). Further simulation details and rigorous evaluations across different environments have been added to the supplementary materials. The code for planner comparison is available at <https://github.com/jatinarora30/safeplan>. The Nav2 version linked to compare on the actual robot package is available at https://github.com/jatinarora30/nav2_safeplan.

Table 3: Planners comparison in Sparse Env(Map 1)

| Planner | Time (ms) | Clearance (cm) | Turn (deg) | Length (m) | SR (in percent) | OSI |
|------------|-----------|----------------|------------|------------|-----------------|-------|
| Voronoi | 23.63 | 99.06 | 74.68 | 33.39 | 84 | 0.583 |
| A* | 124.01 | 25.47 | 352.88 | 33.45 | 100 | 0.271 |
| RRT | 1129.63 | 76.06 | 3624.14 | 41.47 | 89 | 0.366 |
| CBF-RRT | 897.02 | 71.77 | 3552.70 | 40.95 | 91 | 0.386 |
| FS | 2878.66 | 94.48 | 343.39 | 33.25 | 100 | 0.587 |
| SDF-A* | 5283.81 | 277.07 | 2610.31 | 38.45 | 100 | 0.790 |
| Opt-A* | 391.41 | 51.39 | 73.49 | 35.92 | 100 | 0.386 |
| UPP (Ours) | 279.83 | 42.04 | 450.08 | 33.56 | 100 | 0.575 |

On analyzing the results for the sparse environment (Table 3) and visualizing the generated paths (Fig.4), several trends become evident. A* achieves a short path length (33.45 m), but also exhibits the lowest minimum clearance among all planners, making it the least safe

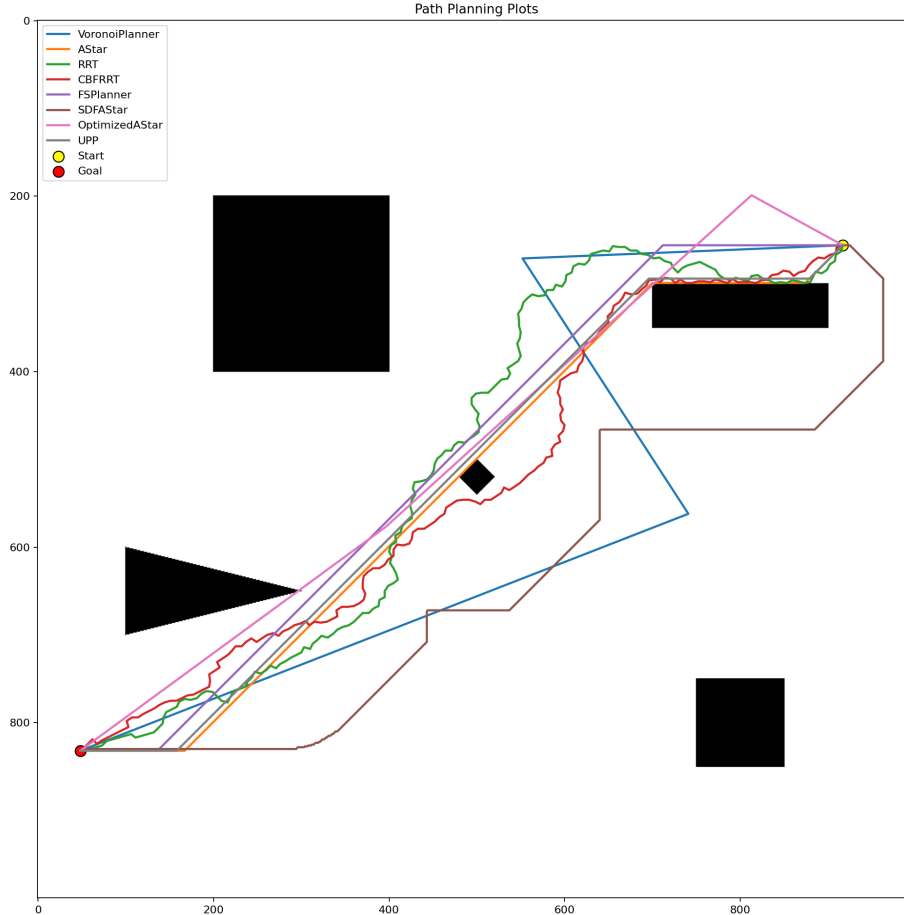


Figure 4: Planner comparison for random start and goal for Map 1

option. Conversely, SDF-A* produces the highest safety margin, although at the cost of approximately 15% longer path length compared to the optimal. Thus, each method predominantly optimizes a single objective, either safety or optimality, without balancing the trade-off.

Voronoi planning provides both high clearance and near-optimal length, but its inability to reliably construct Voronoi diagrams in certain grid structures limits its practical applicability. RRT and CBF-RRT demonstrates high success rates; however, its sampling-based nature leads to extremely high turning angles and longer paths, indicating reduced smoothness and increased controller effort. Turning angle is an important metric for robot navigation because it directly reflects path smoothness and the ease of execution by a physical robot. FS Planner (FS) and Optimized A* (Opt-A*) performs similarly to UPP in terms of optimality with consistent safety margins. UPP achieves a path length of 33.56 m, only a 0.5% deviation from A* while maintaining higher clearance. Even though the clearance is significantly less than SDF-A*, FS, it is more computationally expensive than these algorithms. This demonstrates that UPP effectively balances optimality and safety at a considerably lower computational cost than other safety-aware planners.

To justify the effectiveness of the proposed OptiSafe Index (OSI), we analyze how it cap-

tures the joint balance between safety and optimality. As shown in Table 3, A* exhibits the lowest path length but a low OSI value of 0.271, reflecting its strong bias toward optimality with minimal emphasis on safety. Voronoi achieves a higher OSI of 0.583 because it maintains both good clearance and near-optimal length. RRT and CBF-RRT yield relatively low OSI values despite high minimum clearance, as their long and non-smooth paths significantly reduce their overall safety optimality balance.

SDF-A* obtains the highest OSI (0.790), owing to its consistently high-clearance paths with only moderate deviation (approximately 15%) from the optimal path length. UPP achieves an OSI of 0.575, substantially higher than A* and comparable to FS Planner and SDF, maintaining near-optimal path length, at considerably low computation cost. This indicates that UPP offers one of the best practical trade-offs among the evaluated planners for practical uses, achieving a balanced combination of safety and optimality.

Table 4: Planners comparison in Cluttered Env(Map 2)

| Planner | Time (ms) | Clearance (cm) | Turn (deg) | Length (m) | SR (in percent) | OSI |
|------------|-----------|----------------|------------|------------|-----------------|------|
| Voronoi | 49.33 | 0.20 | 2.57 | 0.51 | 2 | 0.02 |
| A* | 643.09 | 6.88 | 264.80 | 39.29 | 100 | 0.22 |
| RRT | 2365.59 | 7.27 | 4457.76 | 50.28 | 77 | 0.27 |
| CBF-RRT | 2954.64 | 9.93 | 4138.33 | 48.09 | 74 | 0.29 |
| FS Planner | 4548.80 | 18.53 | 321.89 | 39.19 | 100 | 0.36 |
| SDF-A* | 6410.51 | 118.42 | 1112.94 | 43.37 | 100 | 0.85 |
| Opt-A* | 1418.49 | 35.10 | 161.90 | 45.27 | 100 | 0.38 |
| UPP (Ours) | 1158.61 | 25.44 | 433.57 | 39.62 | 100 | 0.94 |

On further analyzing the results for the cluttered environment (Table 4) and visualizing the generated paths (Fig. 5), several important differences emerge compared to the sparse case. Voronoi performs poorly in this map, achieving a success rate of only 2% due to its inability to generate valid medial-axis structures in heavily cluttered regions. A* maintains low path length, but produces extremely low minimum clearance (0.2 cm), indicating that it frequently drives through narrow passages with minimal safety margin.

Sampling-based planners (RRT and CBF-RRT) again show very high turning angles and long, non-smooth paths, which are undesirable for real robot execution. Their success rates also degrade substantially in this cluttered environment. SDF-A* achieves the highest clearance, but produces paths that are approximately 10% longer than the optimal. In contrast, UPP maintains a high success rate and achieves a path length of 39.62 m (approx 1% optimal deviation) with a minimum clearance of 25.44 cm, striking a strong balance between safety and path optimality. UPP’s has the highest OSI score of 0.94 . This highlights UPP’s robustness in cluttered scenarios, where it successfully avoids narrow unsafe regions while keeping the path length near optimal.

To further validate the OptiSafe Index (OSI) in the cluttered environment, we examine how it reflects the balance between safety and optimality across planners (Table 4). Voronoi achieves a very low OSI of 0.02, leading to unreliable behavior in densely cluttered maps. A* again shows a moderate OSI (0.22), capturing the fact that its paths exhibit extremely low clearance and therefore low safety. Sampling-based planners (RRT and CBF-RRT) also

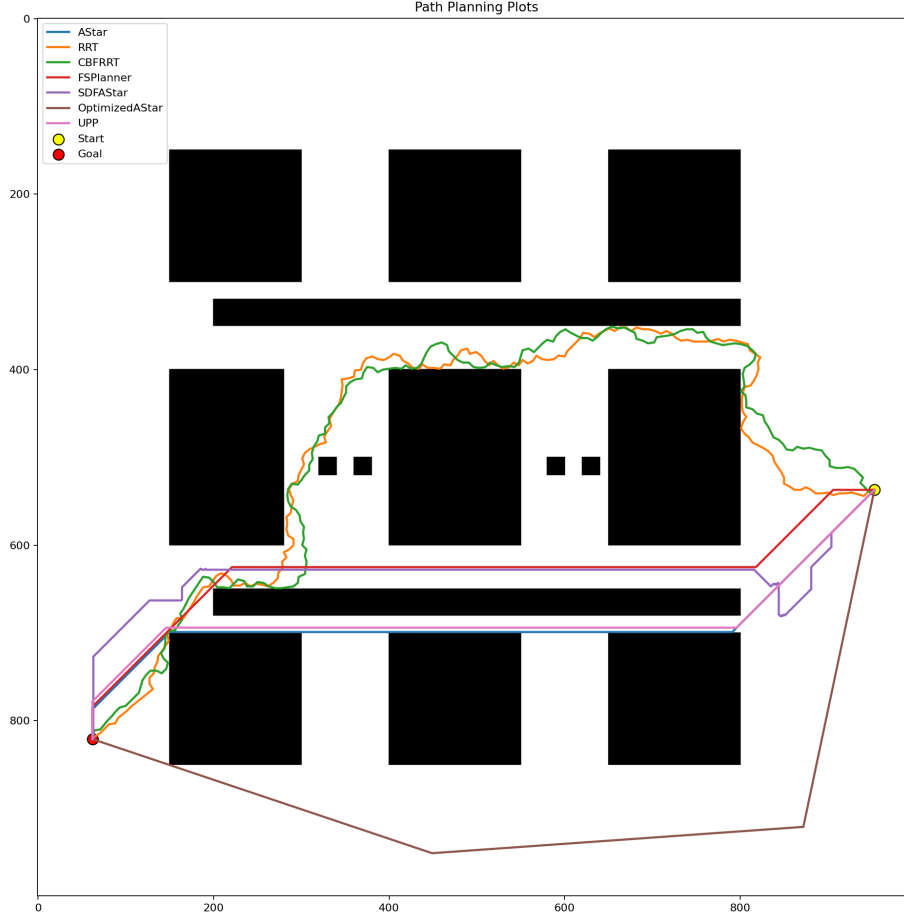


Figure 5: Planner comparison for random start and goal for Map 2

obtain low OSI values, since their high turning angles and long path lengths overshadow their minimal clearances, leading to poor safety-optimality trade-offs.

SDF-A* attains the second-highest OSI (0.85) by producing high-clearance paths with moderate deviation from optimal length, confirming its strong emphasis on safety in cluttered regions. UPP achieves the highest OSI of 0.94, maintaining significantly better near-optimal path length. This demonstrates that UPP consistently balances safety and optimality in a manner aligned with OSI, even in highly cluttered scenarios where traditional planners struggle to maintain both objectives simultaneously.

As shown in the tables, SDF-A* and UPP attain comparable OptiSafe Index values in a sparse environment, with UPP requiring considerably less time. While UPP achieves the highest OptiSafe index in a cluttered environment, balancing both safety and optimality in a considerable manner.

6. Hardware experiments

6.1. Experimental setup

In this section, we present the results of experiments on the proposed method using a hardware test bench for a TurtleBot robot. The TurtleBot was equipped with a LiDAR

sensor for Simultaneous Localization and Mapping (SLAM), and ROS2-humble served as the interface. Mapping was done using the cartographer package in the lab, resulting in an area with few obstacles. The benchmark code was integrated as a global planner in the Nav2 package on the Turtlebot, and DWA was used as a local planner for obstacle avoidance.

6.2. Results and analysis

Table 5: Average performance over 5 runs.

| Planner | Length (m) | Clearance (cm) | Turn (deg) |
|------------|------------|----------------|------------|
| UPP (Ours) | 3.75 | 6.68 | 341.7 |
| FSPlanner | 3.63 | 6.44 | 365.6 |
| SDF* | 3.59 | 6.12 | 387.8 |

Table 5 summarizes the average path length, minimum obstacle clearance, and total turning angle over five runs for UPP and the compared planners. For experimentation purposes, top-performing safety planners have been evaluated. The hardware results reveal a performance gap compared to the simulation. UPP’s path length (3.75m) exceeds both FSPlanner and SDF-A* by 3-4%, while simulation showed <1% optimality deviation. We consider the sim-to-real gap a priority for possible future work. However, UPP consistently maintains greater minimum obstacle clearance and lower turning effort, resulting in safer and smoother trajectories. This behavior aligns with UPP’s objective to prioritize safety-aware navigation while allowing a controlled deviation from the shortest path. Notably, the increase in path length remains marginal relative to the gains in safety and smoothness, indicating a favorable trade-off for navigation in cluttered environments where conservative motion is desirable.

7. Conclusions, Future Work and Limitations

In this paper, we have proposed a Unified Path Planner, a unified framework for optimality and safety in planning, compared to other algorithms that primarily focus on either optimality or safety. The flexibility in UPP allows auto-tuning at runtime based on the path’s direction towards the goal and stalled safety. The bounded suboptimality cost is a function of dimension, increasing with higher dimensions. Future work could include reducing computational cost in higher dimensions and improving UPP’s ability to handle dynamic obstacles. We have also presented the OptiSafe Index, a normalized score that defines the balance and strength between optimality and safety. Extensive simulations and experiments have done for planners to evaluate across various metrics. It has been observed that UPP was able to balance optimality and safety in various environments.

References

- Paden, B., Cap, M., Yong, S. Z., Yershov, D., & Frazzoli, E., *A Survey of Motion Planning and Control Techniques for Self-Driving Urban Vehicles*, IEEE Transactions on Intelligent Vehicles, vol. 1, no. 1, pp. 33–55, 2016.

- Li, C., Wang, J., Wang, X., & Zhang, Y., *A model based path planning algorithm for self-driving cars in dynamic environment*, Proc. Chinese Automation Congress (CAC), pp. 1123–1128, 2015.
- Lee, U., Yoon, S., Shim, H., Vasseur, P., & Demonceaux, C., *Local path planning in a complex environment for self-driving car*, Proc. IEEE Cyber Technology Conference, pp. 445–450, 2014.
- Dai, Y., Xiang, C., Zhang, Y., Jiang, Y., Qu, W., & Zhang, Q., *A Review of Spatial Robotic Arm Trajectory Planning*, Aerospace, vol. 9, no. 7, p. 361, 2022.
- Korayem, M. H., Nohooji, H. R., & Nikoobin, A., *Path Planning of Mobile Elastic Robotic Arms by Indirect Approach of Optimal Control*, International Journal of Advanced Robotic Systems, vol. 8, no. 1, 2011.
- Kim, B. K. & Shin, K. G., *Minimum-time path planning for robot arms and their dynamics*, IEEE Transactions on Systems, Man, and Cybernetics, vol. SMC-15, no. 2, pp. 213–223, 1985.
- Klanke, S., Lebedev, D., Haschke, R., Steil, J., & Ritter, H., *Dynamic Path Planning for a 7-DOF Robot Arm*, Proc. IEEE/RSJ IROS, pp. 3879–3884, 2006.
- Bortoff, S. A., *Path planning for UAVs*, Proc. American Control Conference, vol. 1, pp. 364–368, 2000.
- Hvezda, J., Rybecky, T., Kulich, M., & Preucil, L., *Context-Aware Route Planning for Automated Warehouses*, Proc. ITSC, pp. 2955–2960, 2018.
- Vivaldini, K. C. T., Galdames, J. P. M., Bueno, T. S., Araujo, R. C., Sobral, R. M., Becker, M., & Caurin, G. A. P., *Robotic forklifts for intelligent warehouses: Routing, path planning, and auto-localization*, Proc. IEEE ICIT, pp. 1463–1468, 2010.
- Warren, C. W., *Fast path planning using modified A* method*, Proc. IEEE ICRA, pp. 662–667, 1993.
- Nash, A., & Koenig, S., *Any-Angle Path Planning*, AI Magazine, vol. 34, no. 4, pp. 85–107, 2013.
- Stentz, A., *Optimal and efficient path planning for partially-known environments*, Proc. IEEE ICRA, pp. 3310–3317, 1994.
- Noreen, I., Khan, A., & Habib, Z., *Optimal Path Planning using RRT* based Approaches: A Survey*, IJACSA, vol. 7, no. 11, 2016.
- Nasir, J., Islam, F., Malik, U., Ayaz, Y., Hasan, O., Khan, M., & Muhammad, M. S., *RRT*-SMART: A Rapid Convergence Implementation of RRT**, IJARS, vol. 10, no. 7, 2013.
- Wu, Z., Meng, Z., Zhao, W., & Wu, Z., *Fast-RRT: A RRT-Based Optimal Path Finding Method*, Applied Sciences, vol. 11, no. 24, p. 11777, 2021.

- LaValle, S. M., *Planning Algorithms*, Cambridge University Press, 2006.
- Jafarzadeh, H., & Fleming, C., *An Exact Geometry-Based Algorithm for Path Planning*, International Journal of Applied Mathematics and Computer Science, vol. 28, no. 3, pp. 493–504, 2018.
- Ayawli, B. B. K., Mei, X., Shen, M., Appiah, A. Y., & Kyeremeh, F., *Mobile Robot Path Planning in Dynamic Environment Using Voronoi Diagram and Computational Geometry Technique*, IEEE Access, vol. 7, pp. 86026–86040, 2019.
- Hwang, Y. K., & Ahuja, N., *A potential field approach to path planning*, IEEE Transactions on Robotics and Automation, vol. 8, no. 1, pp. 23–32, 1992.
- Rostami, S. M. H., Sangaiah, A. K., Wang, J., & Liu, X., *Obstacle avoidance of mobile robots using modified artificial potential field algorithm*, EURASIP JWCN, 2019.
- Azzabi, A., & Nouri, K., *An advanced potential field method proposed for mobile robot path planning*, Transactions of the Institute of Measurement and Control, vol. 41, no. 11, pp. 3132–3144, 2019.
- Chu, L., Wang, Y., Li, S., Guo, Z., Du, W., Li, J., & Jiang, Z., *Intelligent Vehicle Path Planning Based on Optimized A* Algorithm*, Sensors, vol. 24, no. 10, p. 3149, 2024.
- Manjunath, A., & Nguyen, Q., *Safe and Robust Motion Planning for Dynamic Robotics via Control Barrier Functions*, Proc. CDC, pp. 2122–2128, 2021.
- Wang, H., Lin, Y., Zhang, W., Ye, W., Zhang, M., & Dong, X., *Safe Autonomous Exploration and Adaptive Path Planning Strategy Using Signed Distance Field*, IEEE Access, vol. 11, pp. 144663–144675, 2023.
- Cobano, J.A., Merino, L., & Caballero, F., *Exploiting Euclidean Distance Field Properties for Fast and Safe 3D Planning with a Modified Lazy Theta**, arXiv preprint arXiv:2505.24024, 2025.
- Hart, P., Nilsson, N., & Raphael, B., *A Formal Basis for the Heuristic Determination of Minimum Cost Paths*, IEEE Transactions on Systems Science and Cybernetics, vol. 4, no. 2, pp. 100–107, 1968.